Safety evaluation of station settlement pipeline based on physical-information fusion

Cheng Xie [1] , Tiefeng Shi [1] , Yao Wang [1] , Liwen Chen [2,3,4], Yinan Zhang [2,3,4], * Shaohua Dong [2,3,4]

[1] Southern China Branch of PipeChina. Guangdong 510623, China
[2] College of Safety and Marine Engineering, China University of Petroleum (Beijing) Beijing 102249, China
[3] Key Laboratory of Oil and Gas Safety and Emergency Technology, Ministry of Emergency Management, Beijing 102249, China
[4] Pipeline Technology and Safety Research Center, China University of Petroleum (Beijing), Beijing 102249, China

Corresponding author E-mail : shdong@cup.edu.cn

Abstract. The foundation of the station built in the coastal area is often weak in lithology, and uneven settlement is easy to occur in the station. The safety risk system of station pipeline under uneven settlement involves many elements and complex components. Therefore, to evaluate the safety level of station pipeline under land subsidence, it is necessary to construct a complete, comprehensive, scientific and effective safety evaluation index system for station pipeline settlement. Combined with the formation mechanism of uneven ground settlement, PS-InSar technology is used to monitor the amount of ground settlement, and the influencing factors of station ground settlement and pipeline risk are identified and analyzed. The safety evaluation factor set of station pipeline settlement is determined, and the index system is established. By physical-information fusion, an evaluation model of station pipeline settlement safety level based on analytic hierarchy process and entropy weight method is proposed.

Keywords :S-InSAR ; oil and gas station ; land subsidence monitoring, safety evaluation

1 Introduction

The stations built in coastal areas are prone to shear failure of pipelines due to uneven settlement of the ground. The factors affecting the safety of station pipelines under the action of land subsidence are multi-level and multi-faceted. Therefore, it is of great significance to improve the safety of station pipelines during operation by analyzing and determining the influencing factors, scientifically constructing the safety evaluation system of station pipeline settlement, and establishing the evaluation model of station pipeline settlement based on physical-information fusion.

Q. Gao et al. (eds.), *Proceedings of the 2024 7th International Conference on Structural Engineering and Industrial Architecture (ICSEIA 2024)*, Atlantis Highlights in Engineering 30,
https://doi.org/10.2991/978-94-6463-429-7_13

At present, there are many surface monitoring methods for land subsidence. Precision leveling and GPS monitoring technology are high-precision point measurement methods with high precision, but it is difficult to achieve wide-area continuous monitoring[1,2]. UAV low-altitude remote sensing has the advantages of flexibility and high efficiency in ground monitoring, but its monitoring accuracy is not high, and it is easy to be restricted by weather factors[3,4]. The three-dimensional lidar technology can obtain the point cloud data of the monitoring object, covering the deformation information of a single monitoring point and the overall deformation trend of the monitoring object. However, the observation accuracy of the three-dimensional lidar will be greatly reduced with the increase of the monitoring distance, and its observation distance is limited[5,6]. Synthetic Aperture Radar (InSAR) technology uses the relationship between the phase difference of the two observed signals and the spatial geometric relationship between the radar and the monitoring object[7,8] to obtain the ground deformation information of the monitoring area.The monitoring accuracy can reach millimeter level, which has the advantages of high precision, all-day, large range and not easy to be affected by weather conditions[9,10].Compared with other traditional deformation monitoring technologies, InSAR technology is the main force of ground deformation monitoring in the new era.

It can be seen from the existing research that there are many deep learning methods used for pipeline safety evaluation, including artificial neural network, fuzzy analytic hierarchy process, Bayesian model, etc.[11-13]. The station pipeline under the action of foundation settlement is a complex system restricted by many factors. The factors affecting the system safety are multi-source, fuzzy and uncertain. In the monitoring and safety evaluation of station pipelines under uneven settlement conditions, the multi-source of monitoring data and safety evaluation indicators should be considered.

In this paper, compared with single source, physical-information fusion data of station pipeline can increase system reliability, make up for the inaccuracy and one-sidedness of single source, and obtain more accurate and comprehensive information of station pipeline[14-16].

2 Acquisition of pipeline stress data

In this paper, a high-precision pipeline remote stress and strain monitoring system is constructed for data acquisition.

The stress of the pipeline is monitored, and the obtained stress data can directly reflect the influence of land subsidence on the pipeline. The vibrating wire strain gauge is a common stress measurement sensor. The TFL-S-BM15 vibrating wire surface strain gauge is used to obtain the circumferential 0° -90° -135° -270° strain data of the pipeline.

Through the pipeline stress monitoring system, the change trend of pipeline stress monitoring values of monitoring points 1 and 2 from February 23,2022 to January 16,2023 is obtained. It can be seen that with the increase of settlement, the stress of pipeline increases slowly, and the change trend is consistent. The monitoring value of the cross-section stress of the monitoring point is between − 10.124 MPa and 20.713

MPa. It can be seen that the stress of the pipeline monitoring point increases rapidly with the accumulation of ground subsidence from February 2022 to early July 2022. From July 2022 to January 2023, the ground subsidence of the station slowed down, and the stress of the pipeline monitoring point also fluctuated within a certain range and tended to be stable.

3 Acquisition of land subsidence data

3.1 Principle of Permanent Scatterer Synthetic Aperture Radar Interferometry (PS-InSAR)

The core idea of PS-InSAR is to obtain SAR images of the same study area at different times, identify permanent scatterers with stable scattering characteristics, that is, PS points. The influence of spatial and temporal decorrelation on these PS points is very small, and the deformation time series information of the ground study area is obtained by using the phase change of PS points.

3.2 Overview of the study area

The research station is located in the south of the Tropic of Cancer, about 22.84°N, 113.55°E. About 15 kilometers downstream is Humen Estuary, 40 nautical miles from Hong Kong. The station is located at the estuary of the Pearl River and has been eroded by seawater for a long time. Under the influence of current hydrodynamic force, the soft soil develops obviously. The thickness of soft soil layer is more than 40 m, and the maximum thickness is 55 m. The regional geological conditions at the site of the station are poor, the lithology is soft, and land subsidence is easy to occur. The study area belongs to the subtropical monsoon climate, with obvious seasonal rainfall. The precipitation from February 2,2022 to January 16,2023 is about 1925 mm.

3.3 Research data

In April 2014, the European Space Agency (ESA) launched Setinel-1A, the first of two sister satellites in the Sentinel series, for the implementation of the Copernicus program[17,18].

Although the resolution of Setinel-1A radar image data is limited, its revisit period is short, the scanning coverage area is complete, and the data is open to the public. It can be obtained for free by logging on the ESA website of ESA or the Alaska Radar Data Download Center website.Therefore, Setinel-1A radar image data was selected as the ground deformation monitoring data source in the study area [19,20].

Combined with the actual situation and the data acquisition time of the Setinel-1A radar research area, the time range from February 2,2022 to January 16,2023 was selected as the research time range, and the image interval was 12 days. The single look complex image (SLC) was obtained after focusing, radiation correction and processing. The working mode is IW, the polarization mode is VV + VH, a total of 30 scenes of ascending (satellite flying from south to north along the orbit) SAR image, the incident angle is about 39.388 °, the size is about 200G [21,22].

In order to remove the terrain phase reference terrain and the reference geographic coordinate system, the reference DEM data needs to be introduced in the PS-InSAR processing. The Space Shuttle Radar Topographic Mapping Data (SRTM) is jointly mapped by the United States Space Agency (NASA) and the United States Department of Defense National Mapping Agency (NIMA) by carrying the SRTM system on the space shuttle. The relevant ground digital elevation model data has been provided free of charge since 2003, and the data accuracy is high [22-23].

SRTM data are divided into SRTM3 with a spatial resolution of 90 m and SRTM1 with a spatial resolution of 30 m. In this paper, STRM1 DEM data with spatial resolution of 30 m is used. The orbit information is an important part of InSAR processing, because the baseline error caused by the orbit deviation will exist in the interferogram as the residual phase, so it is necessary to introduce the Precise Orbit Ephemerides (POD) data to correct the systematic error caused by the orbit error.

The precision orbit data generates a file every day, and each file covers the whole day and one hour before and after the day. The data positioning accuracy is less than 5 cm and stored in EOF format.

3.4 Data processing

ENVI SARscape software is used to process radar images. The software uses a common raster data format, including binary files and header files. The SAR image and DEM data are converted into SARscape standard data format, namely data file, hdr header file and sml SARscape meta file. Since the data width of the IW working mode reaches 250 km, which is much larger than the research scope, the time-series InSAR processing of 30 complete images takes a long time. In order to improve the processing efficiency, the vector file of the study area is generated, and the SAR image is cut in batches, and the study area after cutting is processed. The SAR image after clipping is shown in Figure 1.

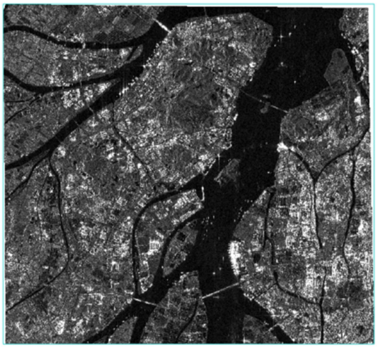

Fig. 1. The average intensity diagram of the cropped SAR image

The maximum spatial baseline of SAR data used is 348 days, and the spatial baseline is distributed between -250 m and 110 m. The single main image method is used to match the interference pairs. The time baseline threshold is set to 365, and the spatial baseline threshold is 2 % of the maximum critical limit. The best main image selected is the SAR image on August 13,2022, generating 29 pairs of interference pairs.

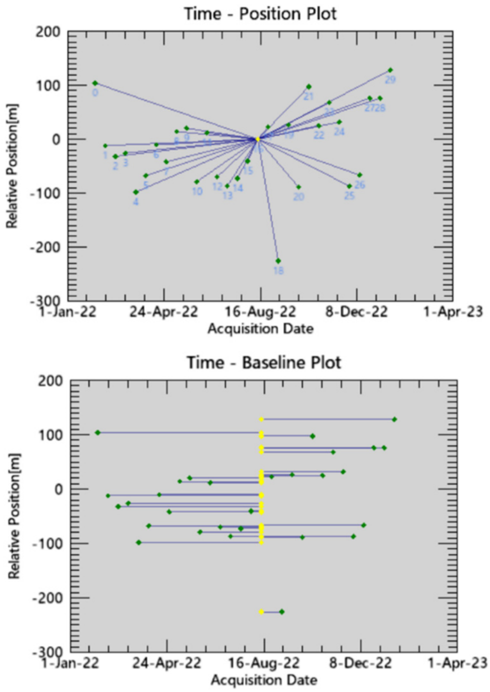

Fig. 2. Schematic diagram of time-location image pairs and diagram of the time baseline

The schematic diagram of the space-time baseline generated by the SAR image on August 13,2022 is shown in Fig.2. The yellow point was the main image, and the green point was the sub-image. The spatial baseline range was −225.957-128.289 m, and the time baseline was −192-156 d. It can be seen from the map that the interference baseline generated by matching the selected main image with other images is generally small. The short space-time baseline is conducive to maintaining the coherence of the interference pair, improving the interference quality, and is conducive to the extraction of subsequent ground deformation.

Interference workflow processing is performed on all image pairs, including interferogram generation, flat-earth effect removal, phase unwrapping, and noise filtering. The 29 sub-images are registered with the main image respectively, and resampled to the main image space to generate interferograms. Four times of sampling is performed in the distance direction to avoid too large spatial baseline, resulting in too dense and blurred interference fringes. The STRM1-30 m DEM data is introduced to remove the terrain phase and generate a differential interferogram. The interferograms of some image pairs are shown in Fig.3. It can be seen that the shorter the space-time baseline, the closer the date is to the main image interference fringes, the more obvious the deformation signal is.

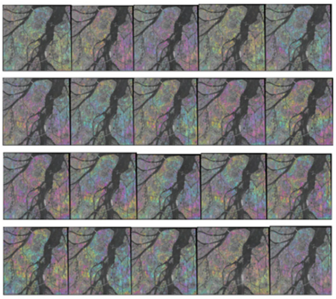

Fig. 3. Interference pattern of partial image pairs

PS points are selected to prepare for the estimation and removal of atmospheric phase. According to the strong reflection characteristics of PS points, high pixel value pixels are selected as PS candidate points by amplitude deviation threshold. These candidate points have better coherence and stability. The final PS points are further selected by using the amplitude deviation index threshold. The points with small amplitude deviation index have better stability in time series.

According to the selected PS points, Delaunay is used to construct the grid. Baselines of adjacent PS points were analyzed. The model is established to estimate the deformation rate and elevation error based on the phase difference between adjacent points. In order to solve this model, the deformation rate increment and elevation error increment are first estimated. Then, the deformation rate and elevation error of all PS points are obtained by integral.

After subtracting the linear deformation phase and the elevation error phase, the remaining phase is the residual phase at each PS point. The residual phase mainly includes the nonlinear deformation phase and the atmospheric phase. The noise phase in the residual phase can be suppressed by spatial low-pass filtering of the residual map, while the ground nonlinear phase exhibits low-frequency characteristics in the time series, and the atmospheric phase exhibits low-frequency characteristics in the time series and low-frequency characteristics in the spatial distribution.Therefore, the residual phase is first subjected to high-pass filtering on the time series, and then low-pass filtering on the space, and the coherence threshold is set to 0.75. The results obtained after filtering can be regarded as the estimation of atmospheric phase, and some of the atmospheric phase time series are shown in Figure 4.

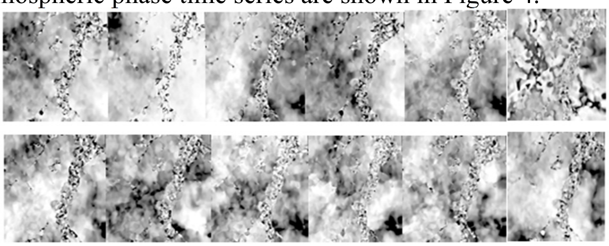

Fig. 4. Time sequence diagram of partial atmospheric delay phase

The processing result of PS-InSAR is the result in the SAR coordinate system. After geocoding, each pixel in the SAR image and the processing result is one-to-one corresponding to its actual geographical location through projection transformation, and the SAR image and interference product in the WGS84 coordinate system are generated, and the vector or grid file is output.

Because the deformation and deformation rate obtained by InSAR technology are in the direction of radar line of sight, according to formula (1), the vertical component of the deformation in the direction of radar line of sight is calculated, and the vertical deformation is the settlement. In the formula, hVD is the vertical deformation, and hLOS is the radar line-of-sight deformation.

$$h_{VD} = \frac{h_{LOS}}{\cos\theta} \tag{1}$$

According to the deformation rate in the vertical direction of the PS point, the settlement rate of the station site in the area is calculated. As shown in figure 5, the vertical deformation rate of the station ground is about-7.929 mm / y. figure 6 is the spatial distribution map of cumulative deformation in the study area. It can be seen that the cumulative settlement of Nansha Station on January 16,2023 is about 11.4 mm compared with that on February 2,2022.

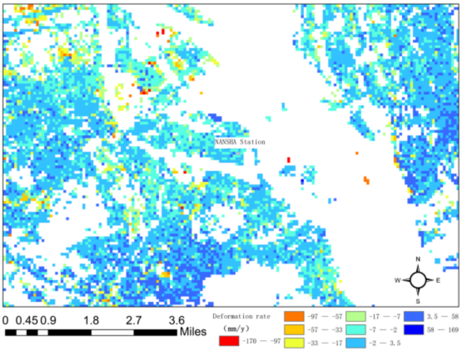

Fig. 5. Graph of average deformation rate

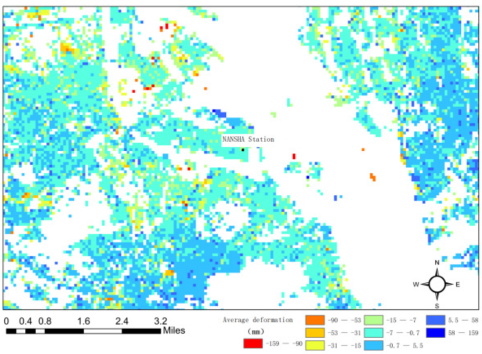

Fig. 6. Graph of cumulative shape variable

4 Safety assessment of station pipeline based on physical-information fusion

4.1 Hierarchical structure model

The safety risk system of station pipeline under uneven settlement involves many elements and complex components. Therefore, to evaluate the safety level of station pipeline under land subsidence, it is necessary to construct a complete, comprehensive, scientific and effective safety evaluation index system for station pipeline settlement. Combined with the formation mechanism of uneven ground settlement, the influencing factors of ground settlement and pipeline risk are identified and analyzed, so as to determine the safety evaluation factor set of station pipeline settlement, establish the index system, and propose a safety level evaluation model of station pipeline settlement based on the combination of physical-information fusion. The hierarchical structure model is shown in Table 1.

Table 1. Hierarchy structure system of safety evaluation index of pipeline settlement

Evaluation objectives	First level indicator layer	Secondary indicator layer
Safety level for settlement of station pipeline	Ground subsidence susceptibility u_1	rainfall u_{11}
		Soil compression coefficient u_{12}
		Ground cumulative deformation u_{13}
		Ground average deformation rate u_{14}
	Vulnerability of station pipeline u_2	Pipeline laying method u_{21}
		Pipeline protection measures u_{22}
		Monitoring value of maximum tensile stress of pipeline u_{23}
		Monitoring value of maximum compressive stress in pipelines u_{24}
		System safety factor u_{25}
	Consequences of Station Pipeline Failure u_3	Flammability of medium u_{31}
		Medium stability u_{32}
		Medium toxicity u_{33}
		Long term hazards of leakage u_{34}
		Station level u_{35}
		Population situation u_{36}

4.2 Entropy weight method

Entropy weight method is an objective weighting method based on statistical theory, which determines the objective weight by the degree of variation of index data. Firstly, the entropy formula proposed by the information scientist Shannon is used to calculate the index information entropy, which indicates the degree of dispersion of the index data. The smaller the information entropy, the greater the degree of index variation, the greater the amount of information contained in the index data, and the greater the weighted value. Suppose that there are m data for n indexes, which form a data matrix $B=(b_{ij})_{m\times n}$.

(1) Data standardization

To standardize the index data, we must first determine the index type, and different indicators have different standardized formulas. After the standardization of the original data matrix R=$(r_{ij})_{m\times n}$, the matrix is obtained.

For positive indicators :

$$r_{ij}=\frac{b_{ij}-\min_j(b_{ij})}{\max_j(b_{ij})-\min_j(b_{ij})} \tag{2}$$

For negative indicators :

$$r_{ij}=\frac{\max_j(b_{ij})-b_{ij}}{\max_j(b_{ij})-\min_j(b_{ij})} \tag{3}$$

(2) Calculate the entropy of the index.

The calculation formula of entropy e_j of index j is :

$$e_j=-k\sum_{i=1}^{m}p_{ij}.\ln p_{ij},e_j\in[0,1],(j=1,2,...,n) \tag{4}$$

$$P_{ij}=\frac{r_{ij}}{\sum_{i=1}^{m}r_{ij}} \tag{5}$$

$$k=\frac{1}{\ln m},k>0 \tag{6}$$

In the formula, Pij is the proportion of the ith data under the index j to all the data of the index j, as the probability in the entropy calculation.

(3) Calculate the weight of the index

The larger the information entropy is, the smaller the information amount of the corresponding index data is, and the smaller the objective weight of the calculated index is. The entropy weight calculation of the index j is shown in the formulas (7) and (8).

$$g_j=1-e_j \tag{7}$$

$$w_j=\frac{g_j}{\sum_{j=1}^{n}g_j} \tag{8}$$

In the formula, gj is the information utility value of index j, and the corresponding weight of each index is obtained after normalization.

4.3 AHP-entropy weight method to determine the index weight

The analytic hierarchy process is a subjective weighting method, and the weights assigned are easily affected by human factors. The entropy weight method is an objective method for calculating weights based on statistical theory. In the calculation process, the weight calculation results may deviate from the actual situation due to the limitations of data samples. Therefore, this paper combines the analytic hierarchy process and the entropy weight method, and synthesizes the subjective weight and the objective weight by multiplication synthesis normalization, so that the subjective weight is corrected by the objective weight, and the result is more scientific and reliable.

The multiplication synthesis normalization formula is shown in formulas. (9) :

$$w_{zi} = \frac{w_i . w_i^{'}}{\sum_{i=1}^{n}(w_i . w_i^{'})}(i = 1,2,...,n) \tag{9}$$

In the formula, wi obtains the subjective weight of index i for the analytic hierarchy process ; w_i' is the objective weight of index i obtained by entropy weight method ; w_{zi} is the comprehensive weight of index i determined by AHP-entropy weight method.

4.4 Safety level division of station pipeline settlement

By scoring the data corresponding to each index and using the comprehensive weight for multi-level linear weighting calculation, the station pipeline safety score can be obtained, and the station pipeline safety score S range is [0,10]. Referring to the method of the Welding Institute (TWI) to divide the risk level, the safety level of the station pipeline is divided into five levels : safety level = { safe, safer, generally safe, less safe, unsafe }.

Safety ($8 < S \le 10$) : The safety level of station pipeline is acceptable, and the risk of pipeline accidents caused by land subsidence is very low, and no measures need to be taken.

Safe ($6 < S \le 8$) : the safety level of station pipeline can be accepted, the level of each index is good, and regular inspection can be carried out.

General safety ($4 < S \le 6$) : The current safety level of the pipeline meets the requirements of normal operation, and risk control measures can be implemented, but a large amount of costs should not be increased. On the basis of comprehensive consideration of economic and technical conditions, the pipeline risk should be reduced and the safety level of pipeline operation should be improved.

Less safe ($2 < S \le 4$) : There are potential safety hazards in the pipeline, and accidents may occur. Preventive measures should be taken to reduce the risk of the pipeline.

Unsafe ($0 \le S \le 2$)

5 Example verification

5.1 Data Acquisition

Through the multi-source data monitoring of the pipeline settlement of the station, the monitoring data of the station for nearly one year is obtained, such as the daily rainfall, ground deformation data and pipeline stress data of the station in the area, and the 15 indexes in the safety evaluation index system of the pipeline settlement of the station.

Through on-site investigation and according to the scoring criteria of various influencing factors, each qualitative index is scored, and all the data of pipeline settlement safety evaluation index of all stations are quantified.

5.2 AHP-entropy weight method to calculate the index weight

(1) Analytic hierarchy process to calculate the index weight

1) Weight calculation of secondary index of pipeline vulnerability

Establish judgment matrix A_2 :

$$A_2 = \begin{bmatrix} 1 & 1/2 & 1/6 & 1/6 & 1/5 \\ 2 & 1 & 1/5 & 1/5 & 1/4 \\ 6 & 5 & 1 & 1 & 2 \\ 6 & 5 & 1 & 1 & 2 \\ 5 & 4 & 1/2 & 1/2 & 1 \end{bmatrix} \tag{10}$$

The weight vector W2 is obtained by normalization :

$$W_2 = (0.0463,0.0682,0.3394,0.3394,0.2067)^T \tag{11}$$

Consistency test :

$$CI = \frac{\lambda_{\max} - n}{n-1} = 0.0172 \tag{12}$$

$$CR = \frac{CI}{RI} = \frac{0.0172}{1.12} < 0.1 \tag{13}$$

Meet the consistency test requirements.

2) Weight calculation of secondary index of pipeline failure consequence

Establish judgment matrix A_3 :

$$A_2 = \begin{bmatrix} 1 & 1 & 1 & 1 & 3 & 2 \\ 1 & 1 & 1 & 1 & 3 & 2 \\ 1 & 1 & 1 & 1 & 3 & 2 \\ 1 & 1 & 1 & 1 & 3 & 2 \\ 1/3 & 1/3 & 1/3 & 1/3 & 1 & 1/2 \\ 1/5 & 1/5 & 1/2 & 1/2 & 2 & 1 \end{bmatrix} \tag{14}$$

The weight vector W3 is obtained by normalization :

$$W_2 = (0.2065,0.2065,0.2065,0.2065,0.0656,0.1084)^T \tag{15}$$

Consistency test :

$$CI = \frac{\lambda_{\max} - n}{n-1} = 0.0018262 \tag{16}$$

$$CR = \frac{CI}{RI} = \frac{0.01862}{1.24} < 0.1 \tag{17}$$

Meet the consistency test requirements.

3) The calculation of the first-level index weight of the station pipeline settlement safety evaluation

Establish judgment matrix A_0 :

$$A_0 = \begin{bmatrix} 1 & 1/2 & 1 \\ 2 & 1 & 2 \\ 1 & 1/2 & 1 \end{bmatrix} \tag{18}$$

The weight vector W0 is obtained by normalization :

$$W_2 = (0.1635,0.5395,0.297)^T \tag{19}$$

Consistency test :

$$CI = \frac{\lambda_{\max} - n}{n-1} = 0.0045675 \tag{20}$$

$$CR = \frac{CI}{RI} = \frac{0.0045675}{0.58} < 0.1 \tag{21}$$

Meet the consistency test requirements.

(2) Entropy weight method to calculate the index weight

1) First-level index weight calculation of station pipeline settlement safety evaluation

The data matrix $B_0 = (b_{ij})$ m×n, m = 323, n = 15 was constructed for 15 secondary indicators. According to the formula (10) ~ formula (21), the corresponding weights of all secondary indexes in the safety evaluation system of station pipeline settlement are calculated. The weight of the first-level index is added by the corresponding weight of the second-level index, and the weight of the first-level index is 1.

2) Weight calculation of secondary index for settlement safety evaluation of station pipeline

According to the formula (10) ~ formula (21), the corresponding weights of all secondary indexes in the ground subsidence susceptibility index in the safety evaluation system of station pipeline settlement are calculated :

$$W_1^{'} = (0.042471128,0.736727927,0.108882006,0.111918938)^T \quad (22)$$

The corresponding weights of all secondary indicators in the pipeline vulnerability index are :

$$W_2^{'} = (0.256650508.0.086024721.0.187887419.0.23305382.0.236383532)^T \quad (23)$$

The corresponding weights of all secondary indicators in the pipeline failure consequence index are :

$$W_3^{'} = (0.479077662.0.311661101.0.030126211.0.042394425\,0.105782695.0.030957905)^T \quad (24)$$

3) Evaluation results of station pipeline settlement

According to the subjective weight and objective weight of each index calculated above, the weight of each index of station pipeline settlement safety evaluation is determined. The scores of some data and the evaluation results of the safety level of station pipeline settlement are shown in Table 2.

Table 2. Evaluation results of station pipeline settlement

	1	2	3	4	5	6	7	8	9
u_{11}	10	10	10	10	10	10	10	10	10
u_{12}	0	5	0	5	5	0	0	0	0
u_{13}	8	10	10	10	10	10	10	10	10
u_{14}	10	0	0	10	10	10	10	0	10
u_{21}	10	0	0	10	10	10	10	0	10
u_{22}	4	4	0	8	4	6	8	6	10
u_{23}	8	8	8	8	10	10	10	10	10
u_{24}	10	10	10	10	10	10	10	10	10
u_{25}	10	10	10	10	10	10	10	10	10
u_{31}	0	6	0	10	6	6	6	6	0
u_{32}	4	6	4	8	6	6	6	6	0
u_{33}	8	8	10	10	8	8	8	8	8
u_{34}	4	4	6	4	4	4	4	4	8
u_{35}	6	4	10	0	8	0	6	10	0
u_{36}	6	8	10	4	4	4	8	10	8
Assessment	safety	safety	safety	safe	safe	safe	safe	safe	safety

6 Conclusion

(1) In this paper, the InSAR interference geometry model is constructed. By setting the spatio-temporal baseline threshold, the influence of spatio-temporal decoherence is

weakened, and the ground time deformation sequence and deformation rate are obtained. PS-InSAR technology is used to monitor the surface deformation of a station, and SAR images from February 2,2022 to January 16,2023 are obtained. Combined with DEM data with 30 m resolution and precision orbit data, the surface deformation information is inverted, and the ground subsidence data of millimeter level are monitored. The ground deformation data and pipeline stress data obtained by monitoring are all important evaluation basis for the safety level of station pipeline settlement.

(2) The influence factors of the safety evaluation of station pipeline settlement are analyzed, and the establishment principle of the evaluation index system is studied. The safety evaluation index of station pipeline settlement is selected from three aspects : the susceptibility of ground subsidence disaster, the vulnerability of station pipeline and the failure consequence of station pipeline, and the safety evaluation index system of station pipeline settlement is established. Referring to the relevant standard specifications and the actual operation of the station, the evaluation criteria and grading thresholds of each index are determined.

(3) The related theories of analytic hierarchy process and entropy weight method are studied. The multiplication normalization is used to combine the analytic hierarchy process and entropy weight method to calculate the comprehensive weight of evaluation indexes at all levels. The safety grade evaluation model of station pipeline based on AHP-entropy weight multi-level comprehensive weight is constructed, and the safety score of station pipeline is obtained. According to the score, the settlement safety of station pipeline is divided into five grades.

Acknowledgments

This work is supported by the National Pipeline Network Group's 2021 Leading Project "Research on Sensing Technology for Oil and Gas Pipeline Lines and Stations"(WZXGL202106) and Risk Warning Technology for Oil and Gas Field Stations Based on Big Data (2021DQ02-0801).

References

1. Zhou C D , Lan H X , Roland Bürgmann, et al. Application of an improved multi-temporal InSAR method and forward geophysical model to document subsidence and rebound of the Chinese Loess Plateau following land reclamation in the Yan'an New District, Remote Sensing of Environment, Volume 279, 2022.
2. Soheil Oruji, Mehrshad Ketabdar, Douglas Moon, et al. Evaluation of Land Subsidence Hazard on Steel Natural Gas Pipelines in California, Upstream Oil and Gas Technology, volume 8, 2022.
3. Wu Y F , Shan Y , Lai Y M , et al. Method of calculating land surface temperatures based on the low-altitude UAV thermal infrared remote sensing data and the near-ground meteorological data, Sustainable Cities and Society, Volume 78, 2022.
4. Liu C , Cao Y J , Yang C , et al. Pattern identification and analysis for the traditional village using low altitude UAV-borne remote sensing: multifeatured geospatial data to sup-

port rural landscape investigation, documentation and management, Journal of Cultural Heritage, Volume 44, 2020, 185-195,
5. Karl Montalban, Dinesh Atchuthan, Christophe Reymann, Bayesian inference of visibility in fog and smoke artificial conditions from 3D-LiDAR point clouds, Journal of Quantitative Spectroscopy and Radiative Transfer, Volume 308, 2023.
6. Chang Y Y , Xiao W , Benjamin Coifman, Using spatiotemporal stacks for precise vehicle tracking from roadside 3D LiDAR data, Transportation Research Part C: Emerging Technologies, Volume 154, 2023,
7. Kristina J. Reinders, Giorgia Giardina, Florian Zurfluh, et al. Proving compliance of satellite InSAR technology with geotechnical design codes. Transportation Geotechnics, Volume 33, 2022.
8. Hari Shankar, Dharmendra Singh, Prakash Chauhan. Investigation of groundwater induced land subsidence in Ludhiana City using InSAR and Sentinel-1 data. Quaternary Science Advances, Volume 13, 2024.
9. Pius Kipngetich Kirui, Björn Riedel, Markus Gerke. Multi-temporal InSAR tropospheric delay modelling using Tikhonov regularization for Sentinel-1 C-band data. ISPRS Open Journal of Photogrammetry and Remote Sensing. Volume 6, 2022.
10. Liu Y , Han S , Xiong L Y , et al. Three-dimensional deformation velocity field and kinematic characteristic of the middle and east parts of Haiyuan fault zone from InSAR and GPS observations, Advances in Space Research, Volume 71, Issue 8, 2023.
11. Ma P F , Zheng Y , Zhang Z J , et al. Building risk monitoring and prediction using integrated multi-temporal InSAR and numerical modeling techniques. International Journal of Applied Earth Observation and Geoinformation,Volume 114, 2022.
12. Afzal Ahmed Soomro, Ainul Akmar Mokhtar, Jundika Candra Kurnia, et al .A review on Bayesian modeling approach to quantify failure risk assessment of oil and gas pipelines due to corrosion, International Journal of Pressure Vessels and Piping, Volume 200, 2022
13. Yang F X. Research on pipeline corrosion rate model based on grey theory and neural network[D]. Beijing: Beijing university of chemical technology, 2020:3-26.
14. He S Y. Study on coupling risk assessment of submarine oil and gas pipeline leakage[D]. Xian:Xi'an university of architecture and technology, 2021:4-10.
15. Li Y Z , Qian X M , Zhang S Y , et. al. Assessment of gas explosion risk in underground spaces adjacent to a gas pipeline, Tunnelling and Underground Space Technology, Volume 131, 2023
16. Wang J Q , Shuai Y, He R Y , et al. Ultimate strain capacity assessment of local buckling of pipelines with kinked dents subjected to bending loads, Thin-Walled Structures, Volume 169, 2021
17. Maryamsadat Hosseini, Samsung Lim, Burned area detection using Sentinel-1 SAR data: A case study of Kangaroo Island, South Australia, Applied Geography, Volume 151, 2023
18. Rasha M. Abou Samra, R.R. Ali, Monitoring of oil spill in the offshore zone of the Nile Delta using Sentinel data, Marine Pollution Bulletin, volume 179, 2022
19. Zhang L. Research on identification and evaluation methods of geological disasters along oil and gas pipelines[D]. Chengdu: Sichuan normal university, 2020:3-15.
20. Ryan A. Ramirez, Gi-Jun Lee, et.al Monitoring of construction-induced urban ground deformations using Sentinel-1 PS-InSAR: The case study of tunneling in Dangjin, Korea, International Journal of Applied Earth Observation and Geoinformation, Volume 108, 2022,
21. Zhang Y J, Heresh F, Falk A, Small baseline InSAR time series analysis: Unwrapping error correction and noise reduction, Computers & Geosciences, Volume 133, 2019,

22. Hu X , Oommen T , Lu Z , et. al. Consolidation settlement of Salt Lake County tailings impoundment revealed by time-series InSAR observations from multiple radar satellites, Remote Sensing of Environment. Volume 202, 2017, 199-209,
23. Yang M L, Paco López-Dekker, Prabu Dheenathayalan, et. al. Mingsheng Liao, Ramon F. Hanssen,On the value of corner reflectors and surface models in InSAR precise point positioning. ISPRS Journal of Photogrammetry and Remote Sensing, Volume 158, 2019, 113-122,